Annotated Bibliography on

Effect of Mineral Dust on Oceanic Productivity

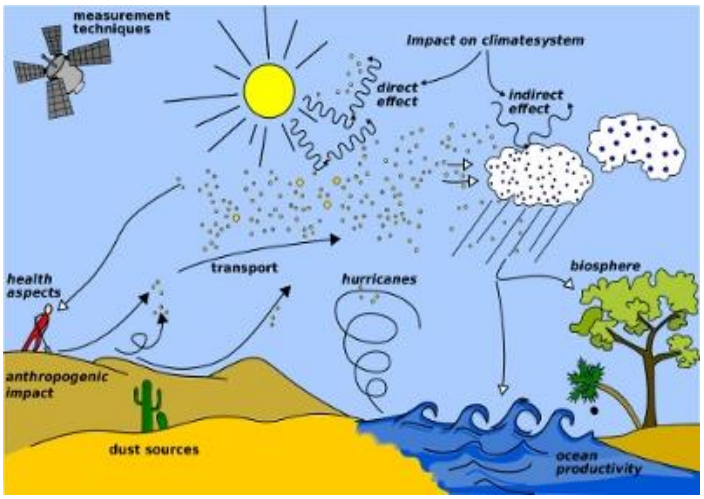

Prepared by:

Fawzia K. Al-Buloushi

November/2022

National Scientific & Technical Information Center
NSTIC

Table of Contents:

Introduction:

Links between oceans and land are innumerable. Each year sand and dust storms (SDS) carry an estimated half a billion tonnes of minerals, nutrients and organic and inorganic matter to oceans from the world's deserts and semideserts. This material helps drive biogeochemical cycles, including nitrogen, carbon and sulphur cycles, which are necessary for Earth system functions. This bibliography contains articles abstracts from 2020-2022.

This benefits EBMMR researchers.

Contact NSTIC to request full-text articles.

Articles Abstract:

1- Baldo, C., Ito, A., Krom, M. D., Li, W., Jones, T., Drake, N., . . . Shi, Z. (2022). Iron from coal combustion particles dissolves much faster than mineral dust under simulated atmospheric acidic conditions. Atmospheric Chemistry and Physics, 22(9), 6045-6066.

Abstract: Mineral dust is the largest source of aerosol iron (Fe) to the offshore global ocean, but acidic processing of coal fly ash (CFA) in the atmosphere could be an important source of soluble aerosol Fe. Here, we determined the Fe speciation and dissolution kinetics of CFA from Aberthaw (United Kingdom), Krakow (Poland), and Shandong (China) in solutions which simulate atmospheric acidic processing. In CFA PM10 fractions, 8%-21.5% of the total Fe was found to be hematite and goethite (dithionite-extracted Fe), and 2%-6.5% was found to be amorphous Fe (ascorbate-extracted Fe), while magnetite (oxalate-extracted Fe) varied from 3%-22%. The remaining 50%-87% of Fe was associated with other Fe-bearing phases, possibly aluminosilicates. High concentrations of ammonium sulfate ((NH4)2SO4), often found in wet aerosols, increased Fe solubility of CFA up to 7 times at low pH (2-3). The oxalate effect on the Fe dissolution rates at pH 2 varied considerably, depending on the samples, from no impact for Shandong ash to doubled dissolution for Krakow ash. However, this enhancement was suppressed in the presence of high concentrations of (NH4)2SO4. Dissolution of highly reactive (amorphous) Fe was insufficient to explain the high Fe solubility at low pH in CFA, and the modelled dissolution kinetics suggest that other Fe-bearing phases such as magnetite may also dissolve relatively rapidly under acidic conditions. Overall, Fe in CFA dissolved up to 7 times faster than in a Saharan dust precursor sample at pH 2. Based on these laboratory data, we developed a new scheme for the proton-and oxalate-promoted Fe dissolution of CFA, which was implemented into the global atmospheric chemical transport model IMPACT (Integrated Massively Parallel Atmospheric Chemical Transport). The revised model showed a better agreement with observations of Fe solubility in aerosol particles over the Bay of Bengal, due to the initial rapid release of Fe and the suppression of the oxalate-promoted dissolution at low pH. The improved model enabled us to predict sensitivity to a more dynamic range of pH changes, particularly between anthropogenic combustion and biomass burning aerosols. © 2022 Clarissa Baldo et al.

2- Boutle, I. A., Joshi, M., Lambert, F. H., Mayne, N. J., Lyster, D., Manners, J., . . . Kohary,

K. (2020). Mineral dust increases the habitability of terrestrial planets but confounds biomarker detection. Nature Communications, 11(1)

Abstract: Identification of habitable planets beyond our solar system is a key goal of current and future space missions. Yet habitability depends not only on the stellar irradiance, but equally on constituent parts of the planetary atmosphere. Here we show, for the first time, that radiatively active mineral dust will have a significant impact on the habitability of Earth-like exoplanets. On tidally-locked planets, dust cools the day-side and warms the night-side, significantly widening the habitable zone. Independent of orbital configuration, we suggest that airborne dust can postpone planetary water loss at the inner edge of the habitable zone, through a feedback involving decreasing ocean coverage and increased dust loading. The inclusion of dust significantly obscures key biomarker gases (e.g. ozone, methane) in simulated transmission spectra, implying an important influence on the interpretation of observations. We demonstrate that future observational and theoretical studies of terrestrial exoplanets must consider the effect of dust. © 2020, Crown.

3- Chen, S. -., Huang, C. -., Kuo, Y. -., Tseng, Y. -., Gu, Y., Earl, K., . . . Liou, K. -. (2021). Impacts of Saharan Mineral Dust on Air-Sea Interaction over North Atlantic Ocean Using a Fully Coupled Regional Model. Journal of Geophysical Research: Atmospheres, 126(4)

Abstract: This study examines the modifications of air-sea coupling processes by dust-radiation-cloud interactions over the North Atlantic Ocean using a high-resolution coupled atmosphere-wave-ocean-dust (AWOD) regional model. The dust-induced mechanisms that are responsible for changes of sea surface temperature (SST) and latent and sensible heat fluxes (LHF/SHF) are also examined. Two 3-month numerical experiments are conducted, and they differ only in the activation and deactivation of dust-radiation-cloud interactions. Model results show that the dust significantly reduces surface downward radiation fluxes (SDRF) over the ocean with the maximum change of 20–30 W m−2. Over the dust plume region, the dust effect creates a low-pressure anomaly and a cyclonic circulation anomaly, which drives a positive wind stress curl anomaly, thereby reducing sea surface height and mixed layer depth. However, the SST change by dust, ranging from −0.5 to 0.5 K, has a great spatial variation which differs from the dust plume shape. Dust cools SST around the West African coast, except under the maximum dust plume ridge, and extends westward asymmetrically along the northern and southern edges of the dust plume. Dust unexpectedly warms SST over a large area of the western tropical North Atlantic and north of the

dust plume. These SST changes are controlled by different mechanisms. Unlike the SST change pattern, the LHF and SHF changes are mostly reduced underneath the dust plume region, though they are different in detail due to different dominant factors, and increased south of the dust plume over the tropic. © 2021. The Authors.

4- Han, Y., Wang, T., Tang, J., Wang, C., Jian, B., Huang, Z., & Huang, J. (2022). New insights into the Asian dust cycle derived from CALIPSO lidar measurements. Remote Sensing of Environment, 272

Abstract: A full understanding of the Asian dust cycle can help with evaluation of the profound impact of mineral dust on human health, the ecosystem, the terrestrial and oceanic biogeochemical cycles, and the weather and climate. The Cloud-Aerosol Lidar with Orthogonal Polarization (CALIOP)-based 3-D dust detection and routine sampling capability, with the accurate dust mass extinction efficiency from Dust Constraints from joint Observational-Modelling-experimental analysis (DustCOMM) dataset, has made it possible to estimate the climatology of Asian dust mass loading (DML) and its transport flux. This study draws on this to provide new insights into the Asian dust cycle, especially the variability of its mass-weighted dust transport central axis (TCA), the contribution of different desert sources to its downstream effects, and the resulting dust budgets in terrestrial and oceanic regions. Dust aerosols emitted from the East Asian and Central Asian deserts together form a heavy dust transport belt stretching from the Taklimakan Desert (TD) and Gobi Desert (GD) to the Pacific Ocean. South Asian dust from the Thar Desert (ThD) can also affect southern China by crossing the Hengduan Mountains and the Yunnan-Guizhou Plateau. The dust TCA is controlled by the terrain of northwest inland China, but shifts in remote regions in the range of 35-50°N due to the western Pacific subtropical high and Aleutian low, and it trend towards a zonal straight line as the altitude increases. The dust transport contribution of the East Asian deserts to the mainland of China and adjacent sea is about 7 times than that of South Asia, with the annual transport fluxes being 214.28 and 30.43 Tg, respectively. The GD dominates the contribution of Asian deserts to the downstream effects and accounts for about 60% of the dust. This can be attributed to its maximum transport flux being near the surface, while the dust transport of the TD and ThD is above 3 km because of the blocking effect of the surrounding terrain. The deposition of Asian dust in the adjacent seas decreases significantly along the dust TCA, with the annual deposition rates being about 40.12, 20.41, and 4.01 g m-2 in the Yellow Sea, Japan Sea and

the Northwest Pacific Ocean, respectively. These new findings and quantification of the Asian dust cycle will help with validation of the simulations provided by global and regional climate models and enable further evaluation of the impact of Asian dust on various related Earth systems.

5- Hartmann, M., Gong, X., Kecorius, S., Van Pinxteren, M., Vogl, T., Welti, A., . . . Stratmann, F. (2021). Terrestrial or marine - indications towards the origin of ice-nucleating particles during melt season in the European Arctic up to 83.7gN. Atmospheric Chemistry and Physics, 21(15), 11613-11636.

Abstract: Ice-nucleating particles (INPs) initiate the primary ice formation in clouds at temperatures above ca. -38gC and have an impact on precipitation formation, cloud optical properties, and cloud persistence. Despite their roles in both weather and climate, INPs are not well characterized, especially in remote regions such as the Arctic. We present results from a ship-based campaign to the European Arctic during May to July 2017. We deployed a filter sampler and a continuous-flow diffusion chamber for offline and online INP analyses, respectively. We also investigated the ice nucleation properties of samples from different environmental compartments, i.e., the sea surface microlayer (SML), the bulk seawater (BSW), and fog water. Concentrations of INPs (NINP) in the air vary between 2 to 3 orders of magnitudes at any particular temperature and are, except for the temperatures above -10gC and below -32gC, lower than in midlatitudes. In these temperature ranges, INP concentrations are the same or even higher than in the midlatitudes. By heating of the filter samples to 95gC for 1ĝ€¯h, we found a significant reduction in ice nucleation activity, i.e., indications that the INPs active at warmer temperatures are biogenic. At colder temperatures the INP population was likely dominated by mineral dust. The SML was found to be enriched in INPs compared to the BSW in almost all samples. The enrichment factor (EF) varied mostly between 1 and 10, but EFs as high as 94.97 were also observed. Filtration of the seawater samples with 0.2ĝ€¯µm syringe filters led to a significant reduction in ice activity, indicating the INPs are larger and/or are associated with particles larger than 0.2ĝ€¯µm. A closure study showed that aerosolization of SML and/or seawater alone cannot explain the observed airborne NINP unless significant enrichment of INP by a factor of 105 takes place during the transfer from the ocean surface to the atmosphere. In the fog water samples with -3.47gC, we observed the highest freezing onset of any sample. A closure study connecting NINP

in fog water and the ambient NINP derived from the filter samples shows good agreement of the concentrations in both compartments, which indicates that INPs in the air are likely all activated into fog droplets during fog events. In a case study, we considered a situation during which the ship was located in the marginal sea ice zone and NINP levels in air and the SML were highest in the temperature range above -10gC. Chlorophyll a measurements by satellite remote sensing point towards the waters in the investigated region being biologically active. Similar slopes in the temperature spectra suggested a connection between the INP populations in the SML and the air. Air mass history had no influence on the observed airborne INP population. Therefore, we conclude that during the case study collected airborne INPs originated from a local biogenic probably marine source. © Author(s) 2021.

6- Liang, L., Han, Z., Li, J., Xia, X., Sun, Y., Liao, H., . . . Zhang, R. (2022). Emission, transport, deposition, chemical and radiative impacts of mineral dust during severe dust storm periods in March 2021 over East Asia. Science of the Total Environment, 852.

Abstract: A Regional Air Quality Model System (named RAQMS) coupled with a developed dust model driven by WRF was applied to synthetically investigate the emission, transport, deposition, budget, and chemical and radiative effects of mineral dust during the severe dust storm periods of 10–31 March 2021. Model results were validated against a variety of ground, vertical and satellite observations, which demonstrated a generally good model ability in reproducing meteorological variables, particulate matter and compositions, and aerosol optical properties. The first dust storm (DS1), which was the severest one since 2010 was originated from the Gobi Desert in southern Mongolia on 14 March, with the dust emission flux reaching 2785 μg m−2 s−1 and the maximum dust concentration exceeding 18,000 μg m−3 in the dust deflation region. This dust storm resulted in remarkably high hourly PM10 observations up to 7506 μg m−3, 1887 μg m−3, and 2704 μg m−3 in Beijing, Tianjin, and Shijiazhuang on 15 March, respectively, and led to a maximum decrease in surface shortwave radiation up to 313.4 W m−2 (72 %) in Beijing. The second dust storm (DS2) broke out in the deserts of eastern Mongolia, with lower dust emission than the first one. The extinction of shortwave radiation by dust aerosols led to a reduction in photolysis rate and consequently decreases in O3 and secondary aerosol concentrations over the North China Plain (NCP), whereas total sulfate and nitrate concentrations consistently increased due to heterogeneous reactions on dust surfaces over the middle reaches of the Yellow River and the NCP

region during DS1. Sulfate and nitrate formation through heterogeneous reactions were enhanced in the dust backflow on 16–17 March by approximately 18 % and 24 % on average in the NCP. Heterogeneous reactions and photolysis rate reduction by mineral dust jointly led to average changes in sulfate, nitrate, ammonium, and secondary organic aerosol (SOA) concentrations by 13.0 %, 13.5 %, −12.3 %, and −4.4 %, respectively, in the NCP region during DS1, larger than the changes in the Yangtze River Delta (YRD). The maximum dry deposition settled in the 7–11 μm size range in downwind land and ocean areas, while wet deposition peaked in the 4.7–7 μm size range in the entire domain. Wet deposition was approximately twice the dry deposition over mainland China except for dust source regions. During 10–31 March, the total dust emission, dry and wet depositions were estimated to be 31.4 Tg, 13.78 Tg and 4.75 Tg, respectively, with remaining 12.87 Tg of dust aerosols (41 % of the dust emission) suspending in the atmosphere or transporting to other continents and oceans.

7- Liebenberg-Enslin, H., von Oertzen, D., & Mwananawa, N. (2020). Dust and radon levels on the west coast of Namibia – What did we learn? Atmospheric Pollution Research, 11(12), 2100-2109

Abstract: The study investigated the potential for adverse health impacts from exposures to inhalable atmospheric dust and radon in the main towns along Namibia's central-western coast. An ambient air quality monitoring network was established at the end of 2016 to measure and track the inhalable dust (specifically PM10) and radon concentrations. Data collected between November 2016 and the end of December 2018 were assessed and selected PM10 samples were analysed for mineral and radionuclide content. In addition, emissions from anthropogenic sources were quantified and simulated using a regional dispersion model. Episodic dust storms associated with easterly winds are a common phenomenon during the winter months in the western part of Namibia. During such events, dust is transported over long distances westwards towards and well into the Atlantic Ocean. In view of the natural and anthropogenic nature of atmospheric dust, the study differentiated between sources of natural dust and those arising as a result of man-made processes. It was found that PM10 concentrations were, on average, higher at the coastal monitoring stations than at the stations located further inland, often exceeding the daily World Health Organisation (WHO) guideline value. Whilst high atmospheric dust concentrations were mostly associated with easterly wind conditions, sea salt was found to be a significant PM10

contributor at the coastal stations. Modelled results, which only included emissions from man-made sources, indicated that these sources contribute very little to the total PM10 concentrations measured at the coastal towns. The radiation exposure doses associated with the inhalation of atmospheric dust and radon were found to be well-below the world-wide average inhalation doses provided by the United Nations Scientific Committee on the Effects of Atomic Radiation (UNSCEAR).

8- MacInnis, J., Chaubey, J. P., Weagle, C., Atkinson, D., & Chang, R. Y. -. (2021). Measurement report: The chemical composition of and temporal variability in aerosol particles at Tuktoyaktuk, Canada, during the Year of Polar Prediction Second Special Observing Period. Atmospheric Chemistry and Physics, 21(18), 14199-14213.

Abstract: The chemical composition, sources, and concentrations of aerosol particles vary on a seasonal basis in the Arctic. While existing research has focused on understanding the occurrence of aerosol particles during the Arctic winter and spring, less is known of their occurrence during the Arctic summer. In this study, atmospheric aerosol particle chemical composition and concentration were determined during July-September 2018 at Tuktoyaktuk, NT, Canada (69.4g ĝ€¯N, 133.0g ĝ€¯W), to coincide with the Year of Polar Prediction's Second Special Observing Period in the Arctic. The chemical composition of fine (PM2.5) and coarse (PM10-2.5) aerosol filter samples suggests the ocean, mineral and/or road dust, and combustion were sources of the sampled aerosol particles. Mass concentrations of PM2 and PM10, estimated from optical particle counter measurements, remained within a similar range during the study. However, elevated mass concentrations coincided with a festival in the community of Tuktoyaktuk, suggesting local human activity was an important source of aerosol particles. Mass concentrations of PM2, which promote negative health effects in humans, were significantly lower at Tuktoyaktuk than the national air quality standard recommended by the government of Canada. These measurements provide an important baseline to compare with future measurements associated with the assessment of aerosol chemistry and air quality in the Arctic. © Copyright:

9- Pagnone, A., Koch, F., Pausch, F., & Trimborn, S. (2021). The Southern Ocean diatom Pseudo-nitzschia subcurvata flourished better under simulated glacial than interglacial ocean conditions: Combined effects of CO2 and iron. PLoS ONE, 16

Abstract: The ‘Iron Hypothesis’ suggests a fertilization of the Southern Ocean by increased dust deposition in glacial times. This promoted high primary productivity and contributed to lower atmospheric pCO2. In this study, the diatom Pseudo-nitzschia subcurvata, known to form prominent blooms in the Southern Ocean, was grown under simulated glacial and interglacial climatic conditions to understand how iron (Fe) availability (no Fe or Fe addition) in conjunction with different pCO2 levels (190 and 290 μatm) influences growth, particulate organic carbon (POC) production and photophysiology. Under both glacial and interglacial conditions, the diatom grew with similar rates. In comparison, glacial conditions (190 μatm pCO2 and Fe input) favored POC production by P. subcurvata while under interglacial conditions (290 μatm pCO2 and Fe deficiency) POC production was reduced, indicating a negative effect caused by higher pCO2 and low Fe availability. Under interglacial conditions, the diatom had, however, thicker silica shells. Overall, our results show that the combination of higher Fe availability with low pCO2, present during the glacial ocean, was beneficial for the diatom P. subcurvata, thus contributing more to primary production during glacial compared to interglacial times. Under the interglacial ocean conditions, on the other hand, the diatom could have contributed to higher carbon export due to its higher degree of silicification.

10- Sakata, K., Kurisu, M., Takeichi, Y., Sakaguchi, A., Tanimoto, H., Tamenori, Y., . . . Takahashi, Y. (2022). Iron (Fe) speciation in size-fractionated aerosol particles in the Pacific Ocean: The role of organic complexation of Fe with humic-like substances in controlling Fe solubility. Atmospheric Chemistry and Physics, 22(14), 9461-9482.

Abstract: Atmospheric deposition is one of the main sources of dissolved iron (Fe) in the ocean surfaces. Atmospheric processes are recognized as controlling fractional Fe solubility (Fesol%) in marine aerosol particles. However, the impact of these processes on Fesol% remains unclear. One of the reasons for this is the lack of field observations focusing on the relationship between Fesol% and Fe species in marine aerosol particles. In particular, the effects of organic ligands on Fesol% have not been thoroughly investigated in observational studies. In this study, Fe species in size-fractionated aerosol particles in the Pacific Ocean were determined using X-ray absorption fine

structure (XAFS) spectroscopy. The internal mixing states of Fe and organic carbon were investigated using scanning transmission X-ray microscopy (STXM). The effects of atmospheric processes on Fesol% in marine aerosol particles were investigated based on the speciation results. Iron in size-fractionated aerosol particles was mainly derived from mineral dust, regardless of aerosol diameter, because the enrichment factor of Fe was almost 1 in both coarse (PM>1.3) and fine aerosol particles (PM1.3). Approximately 80 of the total Fe (insoluble+labile Fe) was present in PM>1.3, whereas labile Fe was mainly present in PM1.3. The Fesol% in PM>1.3 was not significantly increased (2.56±2.53, 0.00-8.50, nCombining double low line20) by the atmospheric processes because mineral dust was not acidified beyond the buffer capacity of calcite. In contrast, mineral dust in PM1.3 was acidified beyond the buffer capacity of calcite. As a result, Fesol% in PM1.3 (0.202-64.7, nCombining double low line10) was an order of magnitude higher than that in PM>1.3. The PM1.3 contained ferric organic complexes with humic-like substances (Fe(III)-HULIS, but not Fe-oxalate complexes), and the abundance correlated with Fesol%. Iron(III)-HULIS was formed during transport in the Pacific Ocean because Fe(III)-HULIS was not found in aerosol particles in Beijing and Japan. The pH estimations of mineral dust in PM1.3 established that Fe was solubilized by proton-promoted dissolution under highly acidic conditions (pH<3.0), whereas Fe(III)-HULIS was stabilized under moderately acidic conditions (pH 3.0-6.0). Since the observed labile Fe concentration could not be reproduced by proton-promoted dissolution under moderately acidic conditions, the pH of mineral dust increased after proton-promoted dissolution. The cloud process in the marine atmosphere increases the mineral dust pH because the dust particles are covered with organic carbon and Na. The precipitation of ferrihydrite was suppressed by Fe(III)-HULIS owing to its high water solubility. Thus, the organic complexation of Fe with HULIS plays a significant role in the stabilization of Fe that was initially solubilized by proton-promoted dissolution.

11- Tuccella, P., Pitari, G., Colaiuda, V., Raparelli, E., & Curci, G. (2021). Present-day radiative effect from radiation-absorbing aerosols in snow. Atmospheric Chemistry and Physics, 21(9), 6875-6893.

Abstract: Black carbon (BC), brown carbon (BrC), and soil dust are the most important radiation-absorbing aerosols (RAAs). When RAAs are deposited on the snowpack, they lower the snow albedo, causing an increase in the solar radiation absorption. The climatic impact associated with

the snow darkening induced by RAAs is highly uncertain. The Intergovernmental Panel on Climate Change (IPCC) Special Report on the Ocean and Cryosphere in a Changing Climate (SROCC) attributes low and medium confidence to radiative forcing (RF) from BrC and dust in snow, respectively. Therefore, the contribution of anthropogenic sources and carbonaceous aerosols to RAA RF in snow is not clear. Moreover, the snow albedo perturbation induced by a single RAA species depends on the presence of other light-absorbing impurities contained in the snowpack. In this work, we calculated the present-day RF of RAAs in snow starting from the deposition fields from a 5-year simulation with the GEOS-Chem global chemistry and transport model. RF was estimated taking into account the presence of BC, BrC, and mineral soil dust in snow, simultaneously. Modeled BC and black carbon equivalent (BCE) mixing ratios in snow and the fraction of light absorption due to non-BC compounds (fnon-BC) were compared with worldwide observations.We showed that BC, BCE, and fnon-BC, obtained from deposition and precipitation fluxes, reproduce the regional variability and order of magnitude of the observations. Global-average all-sky total RAA-, BC-, BrC-, and dust-snow RF were 0.068, 0.033, 0.0066, and 0.012Wm2, respectively. At a global scale, non-BC compounds accounted for 40% of RAA-snow RF, while anthropogenic RAAs contributed to the forcing for 56 %. With regard to non-BC compounds, the largest impact of BrC has been found during summer in the Arctic (C0.13Wm2). In the middle latitudes of Asia, the forcing from dust in spring accounted for 50% (C0.24Wm2) of the total RAA RF. Uncertainties in absorbing optical properties, RAA mixing ratio in snow, snow grain dimension, and snow cover fraction resulted in an overall uncertainty of 50 %/C61 %, 57 %/C183 %, 63 %/C112 %, and 49 %/C77% in BC- , BrC-, dust-, and total RAA-snow RF, respectively. Uncertainty upper bounds of BrC and dust were about 2 and 3 times larger than the upper bounds associated with BC. Higher BrC and dust uncertainties were mainly due to the presence of multiple absorbing impurities in the snow. Our results highlight that an improvement of the representation of RAAs in snow is desirable, given the potential high efficacy of this forcing... © 2021 EDP Sciences.

12- Ventura, A., Simões, E. F. C., Almeida, A. S., Martins, R., Duarte, A. C., Loureiro, S., & Duarte, R. M. B. O. (2021). Deposition of aerosols onto upper ocean and their impacts on marine biota. Atmosphere, 12(6)

Abstract: Atmospheric aerosol deposition (wet and dry) is an important source of macro and

micronu-trients (N, P, C, Si, and Fe) to the oceans. Most of the mass flux of air particles is made of fine mineral particles emitted from arid or semi-arid areas (e.g., deserts) and transported over long distances until deposition to the oceans. However, this atmospheric deposition is affected by anthropogenic activities, which heavily impacts the content and composition of aerosol constituents, contributing to the presence of potentially toxic elements (e.g., Cu). Under this scenario, the deposition of natural and anthropogenic aerosols will impact the biogeochemical cycles of nutrients and toxic elements in the ocean, also affecting (positively or negatively) primary productivity and, ultimately, the marine biota. Given the importance of atmospheric aerosol deposition to the oceans, this paper reviews the existing knowledge on the impacts of aerosol deposition on the biogeochemistry of the upper ocean, and the different responses of marine biota to natural and anthropogenic aerosol input.

13- Wang, Y., Ling, J., Gu, C., Zhou, S., & Jin, X. (2021). Dissolution of Fe from Fe-bearing minerals during the brown-carbonization processes in atmosphere. Science of the Total Environment, 791

Abstract: Previous studies found Fe dissolution in atmosphere correlates to biomass burning, while the underlying mechanisms need to be further investigated. In this study, we reported a laboratory investigation about Fe dissolution behavior of two model Fe-bearing clay minerals of montmorillonite (SWy-2) and illite (IMt-2), and one standard mineral dust of Arizona test dust (AZTD) in atmospheric condition (pH = 2), after the minerals engaging into the brown-carbonization reaction with guaiacol, which is a commonly detected volatile phenol substance in biomass burning. The results show that the pre-brown-carbonization reaction promoted Fe dissolution from all the three minerals, attributing to the reduction of Fe(III) by gaseous guaiacol. The Fe dissolution from SWy-2, IMt-2 and AZTD were also compared under both light and dark conditions to simulate the daytime and nighttime atmospheric processes. As a result, model solar irradiation further promoted Fe dissolution from IMt-2 and AZTD, since both minerals contain moderate photo-reducible Fe(III) oxide or/and Fe(III) oxyhydroxide. The promotive effect of solar irradiation on Fe dissolution from AZTD would be gradually diminished because the photo-reactive Fe(III) is also guaiacol-reducible. Whereas, it was on the contrary for SWy-2 which does not contain the Fe(III) (oxyhydr-)oxide phase. And more dependently, the photo-induced hydroxyl

radical ([rad]OH) on SWy-2 would re-oxidize the formed Fe(II), unless sufficient amount of guaiacol or brown-carbonization products on SWy-2 consumed the [rad]OH and complexed with surface coordinated Fe(III) forming photo-reducible Fe(III). The results of this study suggested the brown carbonization process on minerals would greatly mediate the Fe dissolution behavior from the Fe-bearing mineral dusts in atmosphere. Similar processes might need to be taken into consideration to accurately evaluate the input of Fe from atmosphere to open oceans. © 2021

14- Weis, J., Schallenberg, C., Chase, Z., Bowie, A. R., Wojtasiewicz, B., Perron, M. M. G., Strutton, P. G. (2022). Southern Ocean Phytoplankton Stimulated by Wildfire Emissions and Sustained by Iron Recycling. Geophysical Research Letters, 49(11)

Abstract: Large ash plumes emitted by the 2019–2020 Australian wildfires were associated with a widespread phytoplankton bloom in the iron-limited Pacific sector of the Southern Ocean. In this study, we used satellite observations and aerosol reanalysis products to study the regional phytoplankton community response to wildfire emissions. The bloom was stimulated by pyrogenic iron fertilization and coincided with elevated cellular pigment concentrations, increased photochemical efficiency, and apparent community structural shifts. Physiological anomalies were consistent with previously observed phytoplankton responses to iron stress relief and persisted for up to 9 months. Supported by a regional iron budget, we conclude that the bloom was sustained by iron recycling and episodic inputs of pyrogenic and dust-borne mineral iron. The continuous regeneration of iron was likely facilitated by the bloom's large size, mitigating edge dilution effects, as well as enhanced bioavailability of pyrogenic and mineral iron due to atmospheric and chemical processing during long-range transport. © 2022. The Authors.

15- Woodward, S., Sellar, A. A., Tang, Y., Stringer, M., Yool, A., Robertson, E., & Wiltshire, A. (2022). The simulation of mineral dust in the United Kingdom Earth System Model UKESM1. Atmospheric Chemistry and Physics, 22(22), 14503-14528.

Abstract: Mineral dust plays an important role in Earth system models and is linked to many components, including atmospheric wind speed, precipitation and radiation, surface vegetation cover and soil properties and oceanic biogeochemical systems. In this paper, the dust scheme in the first configuration of the United Kingdom Earth System Model UKESM1 is described, and simulations of dust and its radiative effects are presented and compared with results from the

parallel coupled atmosphere-ocean general circulation model (GCM) HadGEM3-GC3.1. Not only changes in the driving model fields but also changes in the dust size distribution are shown to lead to considerable differences to the present-day dust simulations and to projected future changes. UKESM1 simulations produce a present-day, top-of-the-atmosphere (ToA) dust direct radiative effect (DRE - defined as the change in downward net flux directly due to the presence of dust) of 0.086 W m-2 from a dust load of 19.5 Tg. Under climate change pathways these values decrease considerably. In the 2081-2100 mean of the Shared Socioeconomic Pathway SSP5-8.45 ToA DRE reaches 0.048 W m-2 from a load of 15.1 Tg. In contrast, in HadGEM3-GC3.1 the present-day values of -0.296 W m-2 and 15.0 Tg are almost unchanged at -0.289 W m-2 and 14.5 Tg in the 2081-2100 mean. The primary mechanism causing the differences in future dust projections is shown to be the vegetation response, which dominates over the direct effects of warming in our models. Though there are considerable uncertainties associated with any such estimates, the results presented demonstrate both the importance of the size distribution for dust modelling and also the necessity of including Earth system processes such as interactive vegetation in dust simulations for climate change studies.

16- Xiao, C., Du, Z., Handley, M. J., Mayewski, P. A., Cao, J., Schüpbach, S., . . . Ren, J. (2021). Iron in the NEEM ice core relative to Asian loess records over the last glacial-interglacial cycle. National Science Review, 8(7)

Abstract: Mineral dust can indirectly affect the climate by supplying bioavailable iron (Fe) to the ocean. Here, we present the records of dissolved Fe (DFe) and total Fe (TDFe) in North Greenland Eemian Ice Drilling (NEEM) ice core over the past 110 kyr BP. The Fe records are significantly negatively correlated with the carbon-dioxide (CO2) concentrations during cold periods. The results suggest that the changes in Fe fluxes over the past 110 kyr BP in the NEEM ice core are consistent with those in Chinese loess records because the mineral-dust distribution is controlled by the East Asian deserts. Furthermore, the variations in the dust input on a global scale are most likely driven by changes in solar radiation during the last glacial-interglacial cycle in response to Earth's orbital cycles. In the last glacial-interglacial cycle, the DFe/TDFe ratios were higher during the warm periods (following the post-Industrial Revolution and during the Holocene and last interglacial period) than during the main cold period (i.e. the last glacial maximum (LGM)), indicating that the aeolian input of iron and the iron fertilization effect on the oceans have a non-

linear relationship during different periods. Although the burning of biomass aerosols has released large amounts of DFe since the Industrial Revolution, no significant responses are observed in the DFe and TDFe variations during this period, indicating that severe anthropogenic contamination has no significant effect on the DFe (TDFe) release in the NEEM ice core. © 2020 The Author(s). Published by Oxford University Press on behalf of China Science Publishing & Media Ltd.

17- Yang, S., Wang, Z., Huang, X., Wang, W., Sheng, L., & Zhou, Y. (2021). Meteorological feedback and eco-environmental impact of Asian dust: A simulation study. Atmospheric Environment, 253.

Abstract: Wind-blown dust plays a crucial role in air quality, biogeochemical cycles, and climate change. In East Asia, one of the main dust source regions in the world, dust storms frequently engulf eastern China, with a substantial negative effect on air pollution and the ecological environment. By integrating multiple observations and the online coupled meteorology-chemistry model WRF-Chem, a severe dust storm event originating from the Gobi Desert in early May 2017 is comprehensively analyzed from the perspective of emission estimation, meteorological feedback, and the possible impact on the ecological environment. We optimize the size distribution of dust aerosol by applying local observations to better represent dust emission and regional transport in the model. Both the observations and simulations indicate that the dust storm broke out with PM10 concentrations exceeding 1500 μg/m3 in the source region of the Gobi Desert, and was quickly transported downwind, deteriorating the air quality of cities in northern and eastern China. Moreover, we find that the dust storm significantly perturbed the temperature stratification, since mineral dust is a radiatively active aerosol and can absorb both short- and long-wave radiation. The upper dust layer at an altitude of around 2–3 km became warmer by 1–2 °C while the surface temperature decreased by about 2 °C, making the planetary boundary layer more stable and indirectly aggravating local air pollution near the ground in eastern China. Furthermore, during this event, a large amount of dust deposition increased ocean primary productivity, with the maximum Chlorophyll-a concentration rising from 4 to 14 mg/m3 in the central area of the Yellow Sea. This study highlights the critical impact of Asian dust pollution on air quality and marine ecosystems in downwind areas. © 2021 Elsevier Ltd

18- Yang, T., Chen, Y., Zhou, S., Li, H., Wang, F., & Zhu, Y. (2020). Solubilities and

deposition fluxes of atmospheric Fe and Cu over the Northwest Pacific and its marginal seas. Atmospheric Environment, 239.

Abstract: Atmospheric input is an important exogenous source of Fe and Cu to the surface ocean. Here, we investigated temporal and spatial variations, solubilities, size distributions and deposition fluxes of aerosol Fe and Cu using a unique, new dataset including 3-year observations at Huaniao Island and two cruises during the springtimes of 2015 in the Northwest Pacific (NWP) and of 2017 in the Yellow and East China Seas (YECS). The mean concentrations of soluble aerosol Fe and Cu showed a seasonal variation over Huaniao Island with the highest and lowest values in winter and summer respectively, whilst the total Fe reached the maximum in spring. Their mean concentrations decreased significantly from the coastal island to the YECS and to the NWP. The solubility of aerosol Fe was inversely and positively correlated with crustal element Al and non-sea-salt-SO42- (nss-SO42-), respectively. Moreover, the size distribution of soluble Fe demonstrated major peaks in accord with nss-SO42- and a minor peak associated with total Fe. Based on the size distributions of total and soluble Fe, anthropogenic contribution and acid-enhanced dissolution were firstly estimated to be 61% and 32% of soluble Fe over Huaniao Island, 55% and 30% over the YECS, and 34% and 47% over the NWP, respectively. Unlike the Fe, the solubility of aerosol Cu was more correlated with relative humidity (RH). Our estimates of dry deposition fluxes of soluble Fe and Cu declined greatly from the coastal island 33.3 and 2.9 μg m−2 d−1 to the open Pacific 3.6 and 0.1 μg m−2 d−1, respectively. The fluxes of soluble Fe and Cu could vary asynchronously as a result of different origins and transport paths of air masses. Our concurrent study on aerosol Fe and Cu is very helpful for understanding the atmospheric deposition of bioavailable Fe and Cu to the ocean and their interactive effect on marine phytoplankton. © 2020 Elsevier Ltd

19- Zhao, X., Liu, X., Burrows, S. M., & Shi, Y. (2021). Effects of marine organic aerosols as sources of immersion-mode ice-nucleating particles on high-latitude mixed-phase clouds. Atmospheric Chemistry and Physics, 21(4), 2305-2327.

Abstract: Mixed-phase clouds are frequently observed in high-latitude regions and have important impacts on the surface energy budget and regional climate. Marine organic aerosol (MOA), a natural source of aerosol emitted over 70% of Earth s surface, may significantly modify the properties and radiative forcing of mixed-phase clouds. However, the relative importance of MOA

as a source of icenucleating particles (INPs) in comparison to mineral dust, and MOA s effects as cloud condensation nuclei (CCN) and INPs on mixed-phase clouds are still open questions. In this study, we implement MOA as a new aerosol species into the Community Atmosphere Model version 6 (CAM6), the atmosphere component of the Community Earth System Model version 2 (CESM2), and allow the treatment of aerosol cloud interactions ofMOA via droplet activation and ice nucleation. CAM6 reproduces observed seasonal cycles of marine organic matter at Mace Head and Amsterdam Island when the MOA fraction of sea spray aerosol in the model is assumed to depend on sea spray biology but fails when this fraction is assumed to be constant. Model results indicate that marine INPs dominate primary ice nucleation below 400 hPa over the Southern Ocean and Arctic boundary layer, while dust INPs are more abundant elsewhere. By acting as CCN, MOA exerts a shortwave cloud forcing change of-2.78Wm-2 over the Southern Ocean in the austral summer. By acting as INPs, MOA enhances the longwave cloud forcing by 0.35Wm-2 over the Southern Ocean in the austral winter. The annual global mean net cloud forcing changes due to CCN and INPs of MOA are-0.35 and 0.016Wm-2, respectively. These findings highlight the vital importance for Earth system models to consider MOA as an important aerosol species for the interactions of biogeochemistry, hydrological cycle, and climate change.

20- Zheng, J., Zhang, Z., Garnier, A., Yu, H., Song, Q., Wang, C., . . . Di Biagio, C. (2022). The thermal infrared optical depth of mineral dust retrieved from integrated CALIOP and IIR observations. Remote Sensing of Environment, 270

Abstract: Recent studies have suggested that global climate models tend to underestimate dust particle size in particular, the very coarse mode, leading to an underestimated direct radiative effect (DRE) of dust in the longwave (LW) thermal infrared (TIR) region. However, the magnitude of LW DRE remains highly uncertain, because of limited observations of dust optical depth at the TIR (DAODTIR). This study presents a simple approach to retrieve the DAODTIR over the oceans during nighttime through synergistic use of observations from the Infrared Imaging Radiometer (IIR) and the Cloud-Aerosol Lidar with Orthogonal Polarization (CALIOP), both onboard of the Cloud-Aerosol Lidar and Infrared Pathfinder Satellite Observations (CALIPSO) mission. For each cloud-free dust-laden profile identified by the IIR-CALIOP observation, a Lookup-Table (LUT) of the 10.6 μm IIR band brightness temperatures (BT) difference (dBT) under different DAODTIR

with respect to their dust-free BTs is constructed based on the CALIOP retrieved dust vertical profile and a priori dust scattering properties using a fast radiative transfer model. Then the DAODTIR is retrieved by projecting the IIR-observed dBT on the LUT. Sensitivity studies show that the DAODTIR retrieval at 10.6 μm is more susceptible to the dust particle size distribution (PSD) assumption than dust refractive indices. To estimate the uncertainty caused by PSD assumption, two DAODTIR retrieval products, one based on the dust PSD from the AERONET at Cape Verde and the other on an in situ measured PSD from the recent Fennec campaign, are provided. The retrieval uncertainty is mainly contributed by the BT difference between the observation and simulation using auxiliary atmospheric data. The climatology of the retrieval from 2013 to 2019 shows reasonable spatiotemporal variations of DAODTIR with the global-averaged value of 0.008 and 0.013 based on different pre-assumed dust PSDs. Climatological results agree reasonably well with two independent DAODTIR retrieval products based on the Infrared Atmospheric Sounding Interferometer (IASI) over the active dust transport regions, such as North and Tropical Atlantic ($r = 0.9$ and $r = 0.8$) and Indian Ocean ($r = 0.8$). The seasonal and interannual variation is also well-compared ($r = 0.76$) with AERONET coarse-mode AOD at 97 selected sites. The synergic CALIOP observation allows the retrieved DAODTIR to directly compare with the extrapolated DAODTIR from DAOD in the visible (i.e., 532 nm), which helps evaluate the observational constraints on DAODTIR. Our study clearly reveals that the retrieved DAODTIR from IIR is much less susceptible to various uncertainties than converted results from CALIOP. It also offers a unique prospect of collocated active lidar and passive IR observations for retrieving dust DAODTIR.

Contact NSTIC for Full Text:

Fawzia Al-Buloushi

Fbuloushi@kisr.edu.kw

Ext. 6059

References

Impacts of Sand and Dust Storms on Oceans. (2020). The United Nations Environment Programme. https://wedocs.unep.org/bitstream/handle/20.500.11822/34300/SDO.pdf?sequence=1&isAllowed=y

SDS about | World Meteorological Organization. (n.d.). https://community.wmo.int/sds-about